# Deciphering Water's Dielectric Constant

PRL 117, 185501 (2016) Selected for a Viewpoint in *Physics* PHYSICAL REVIEW LETTERS week ending 28 OCTOBER 2016

## Dielectric Susceptibility of Liquid Water: Microscopic Insights from Coherent and Incoherent Neutron Scattering

A. Arbe,[1] P. Malo de Molina,[1] F. Alvarez,[1,2] B. Frick,[3] and J. Colmenero[1,2,4,*]
[1]*Centro de Física de Materiales (CFM) (CSIC–UPV/EHU)—Materials Physics Center (MPC), Paseo Manuel de Lardizabal 5, 20018 San Sebastián, Spain*
[2]*Departamento de Física de Materiales (UPV/EHU), Apartado 1072, 20080 San Sebastián, Spain*
[3]*Institut Laue-Langevin, 71 Avenue des Martyrs, CS 20156, F-38042 Grenoble Cedex 9, France*
[4]*Donostia International Physics Center, Paseo Manuel de Lardizabal 4, 20018 San Sebastián, Spain*
(Received 16 April 2016; published 24 October 2016)

The analysis of neutron scattering results on H dynamics ($H_2O$) and the dynamic structure factor ($D_2O$) around the intermolecular peak and at intermediate length scales in terms of the susceptibilities reveals three processes (diffusive, local relaxational and vibrational) at frequencies below 3 THz, to which the contributions commonly invoked in dielectric studies can be directly mapped. We achieve a unified description of the results from both techniques, clarifying the nature of the molecular motions involved in the dielectric spectra and their impact on the structural relaxation.

DOI: 10.1103/PhysRevLett.117.185501

https://physics.aps.org/featured-article-pdf/10.1103/PhysRevLett.117.185501

The combination of two spectroscopic techniques reveals the microscopic mechanisms that control the behavior of water's dielectric constant.

https://physics.aps.org/articles/v9/122

A. Arbe and her colleagues combine results from measurements of **dielectric relaxation** and **neutron scattering** to deliver a detailed and unified picture of water dynamics at room temperature. Through dielectric relaxation experiments, the authors characterized the collective relaxation of electrical dipoles that determines the macroscopic dielectric response of water. Thanks to the atomic-scale sensitivity of neutron scattering measurements, they were then able to establish a relationship between molecular dynamics and the dielectric behavior of the liquid.

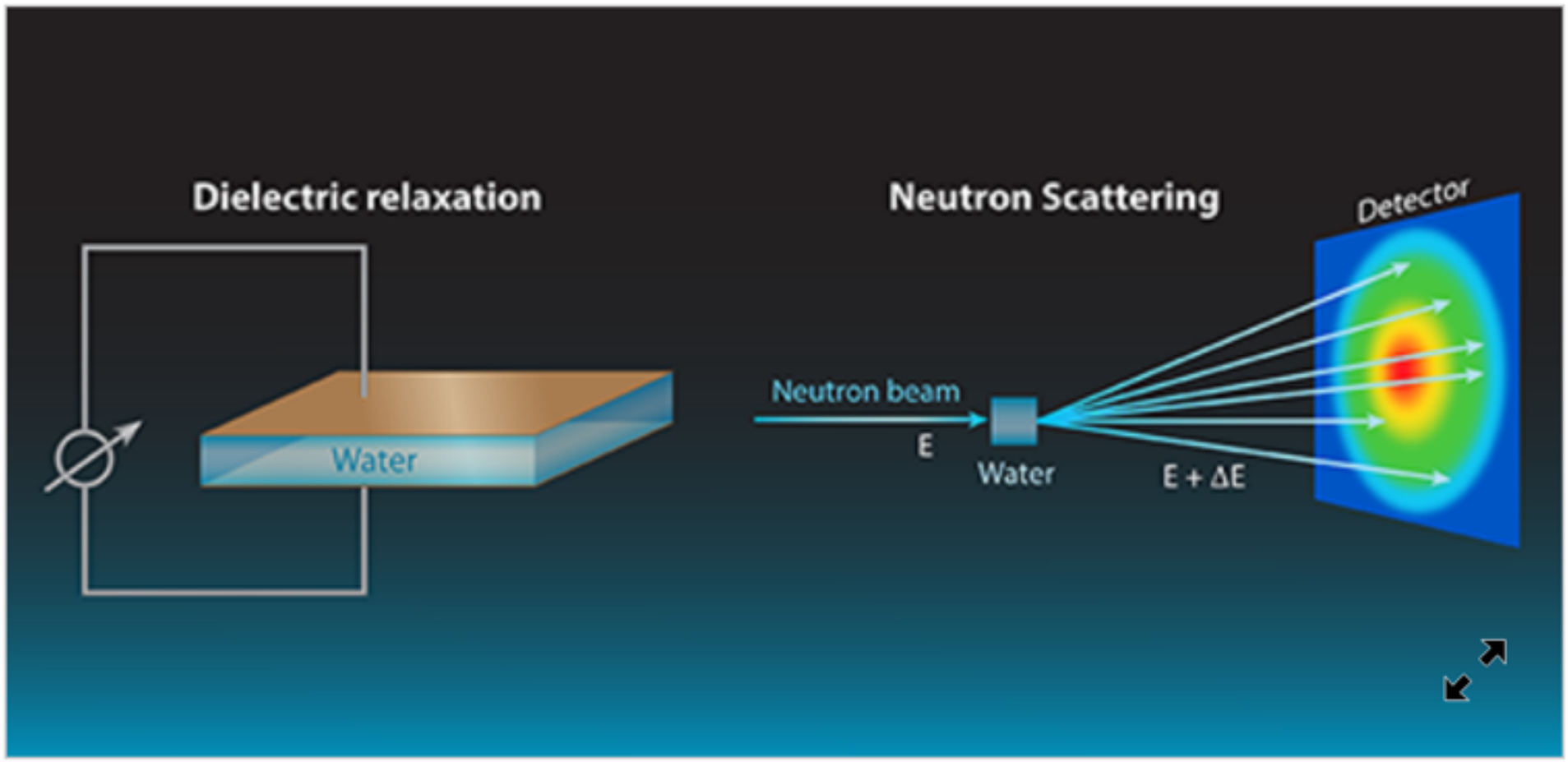


**Figure 1:** Schemes of dielectric relaxation (left) and neutron scattering (right) experiments. Arbe *et al*. [1] combined data of the two techniques to shed light on the molecular mechanisms that control the dielectric constant of water.

# dielectric relaxation at tera-Hz f

Dielectric relaxation, a way to observe water dynamics. The method applies an oscillating electric field to a capacitor containing the liquid, and measures, as a function of the field's frequency, the phase difference between the current and voltage on the capacitor. Extract the dielectric response of the liquid, which is related to the dynamics of the electric dipoles.

They fill the gap between dipolar relaxation and intermolecular stretching vibrations at ≈5 THz, and to have a full picture of the dielectric permittivity

$\varepsilon^{\star}(f)$ of liquid water in a broad frequency range

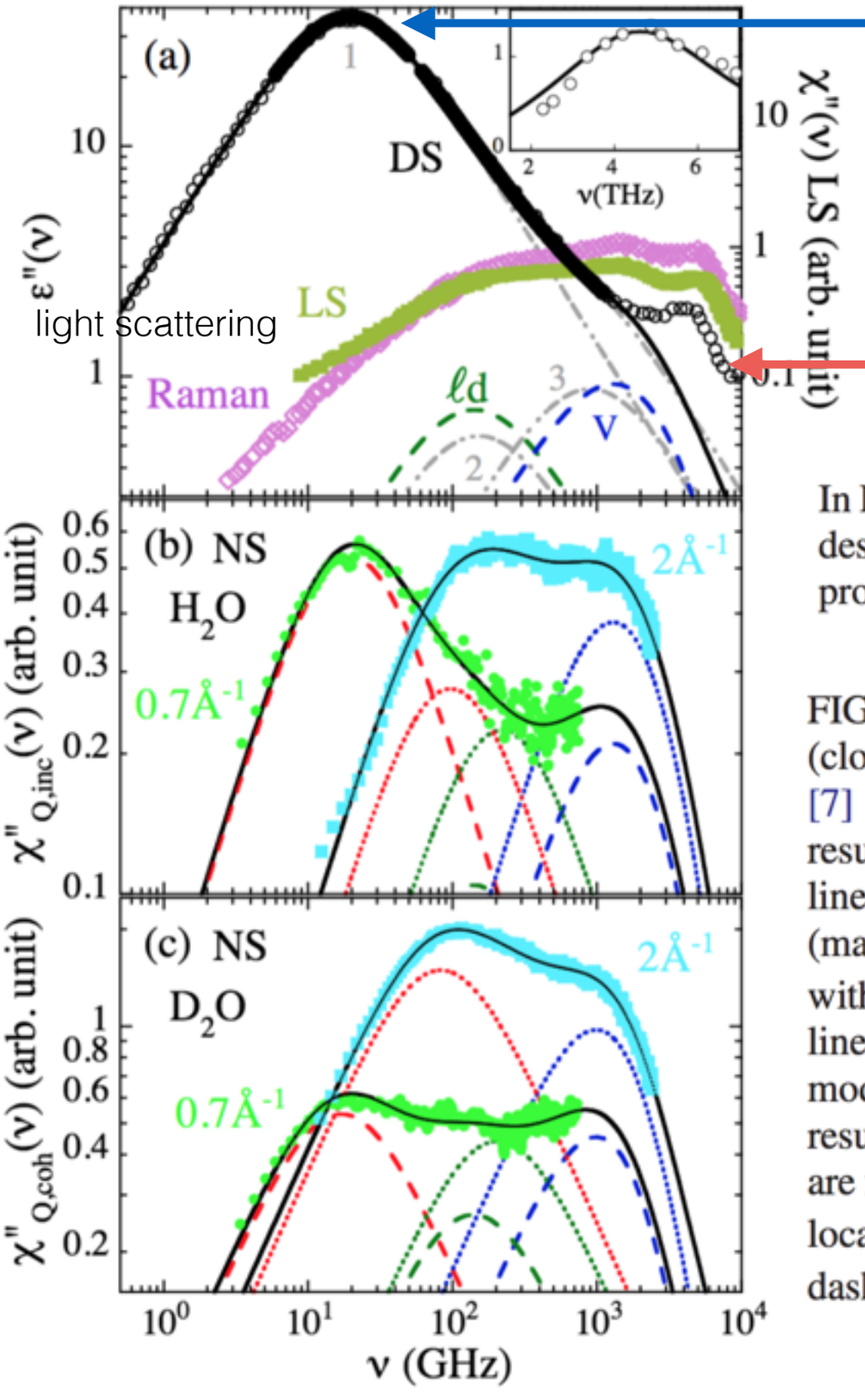


Debye peak, 8.3ps exponential relaxation of collective dipole moment

In Fig. 1(a) we have reproduced the most recently proposed description [5], which includes two additional Debye-like processes with characteristic times $\tau_2 \approx 1$ and $\tau_3 \approx 0.18$ ps.

FIG. 1. Imaginary part of water susceptibility at 298 K. (a) DS (closed [5] and open [2] circles), Raman [6] (diamonds) and LS [7] (squares; $T = 293$ K) results. Lines are fitting curves of DS results from Ref. [5] and respective components: dashed-dotted lines correspond to the fit proposed in Ref. [5] with processes 1 (main Debye), 2, and 3; solid line to the fit obtained in this work with process $d$ for $Q^\star = 0.7$ Å$^{-1}$ and processes $\ell d$ and $V$ (dashed lines). Inset: difference between the DS results and our fit, and model resonance given in Ref. [3] (line). (b) Incoherent NS results. (c) Coherent NS results. In (b) and (c), black solid lines are fits with the three components (red, diffusive; green, effective local; blue, vibrational) to the data at $Q = 0.7$ Å$^{-1}$ (circles, dashed lines) and 2.0 Å$^{-1} \approx Q_{max}$ (squares, dotted lines).

### A. Experimental Details

Ultrapure hydrogenated and deuterated water from Aldrich Chemical Co. Inc. were used without any further purification. The deuterium (D) content in the $D_2O$ sample was 99.85 atom% as determined by proton NMR. Samples were placed in flat aluminum slabs (thicknesses of 1 and 0.1 mm for $D_2O$ and $H_2O$, respectively).

Diffraction with polarization analysis measurements allowing separation of spin-coherent and spin-incoherent contributions [1] were realized at 298 K on the D7 instrument [2] at the Institute Laue-Langevin (ILL) in Grenoble. Using an incident wavelength $\lambda = 3.15$ Å, the wavevector $Q$-range covered by the 132 detectors extends from 0.22 $Å^{-1}$ to 3.8$Å^{-1}$. The raw data were corrected for detector efficiency, flipping ratio, sample container and absorption using ILL standard programs finally obtaining the ratio between the coherent and incoherent differential scattering cross sections as a function of the scattering vector $Q$ ($\hbar\vec{Q}$: momentum transfer).

# I(θ,ω)

The double differential scattering cross sections were measured at 298 K by means of the time-of-flight instrument IN5 [3], also at the ILL, using two wavelengths, $\lambda$=5 and 8Å. Data were corrected for background from sample container and cryostat and detector efficiency. The neutron counts in the time-of-flight channels were then converted to neutron intensity, $I(\theta, \omega)$, as a function of neutron energy transfer, $\hbar\omega$, and scattering angle $\theta$. After interpolating the signal at constant $Q$, the effective $Q$-range was reduced to values between $\approx$0.2 and 1.3Å$^{-1}$ for $\lambda$=8Å, with resolution (HWHM) $\delta\hbar\omega \approx 12\mu$eV ($\approx$ 3GHz), and between $\approx$0.3 and 2.3Å$^{-1}$ for $\lambda$=5Å, with $\delta\hbar\omega \approx 42\mu$eV ($\approx$ 10GHz).

http://journals.iucr.org/j/issues/2009/01/00/db5048/db5048.pdf

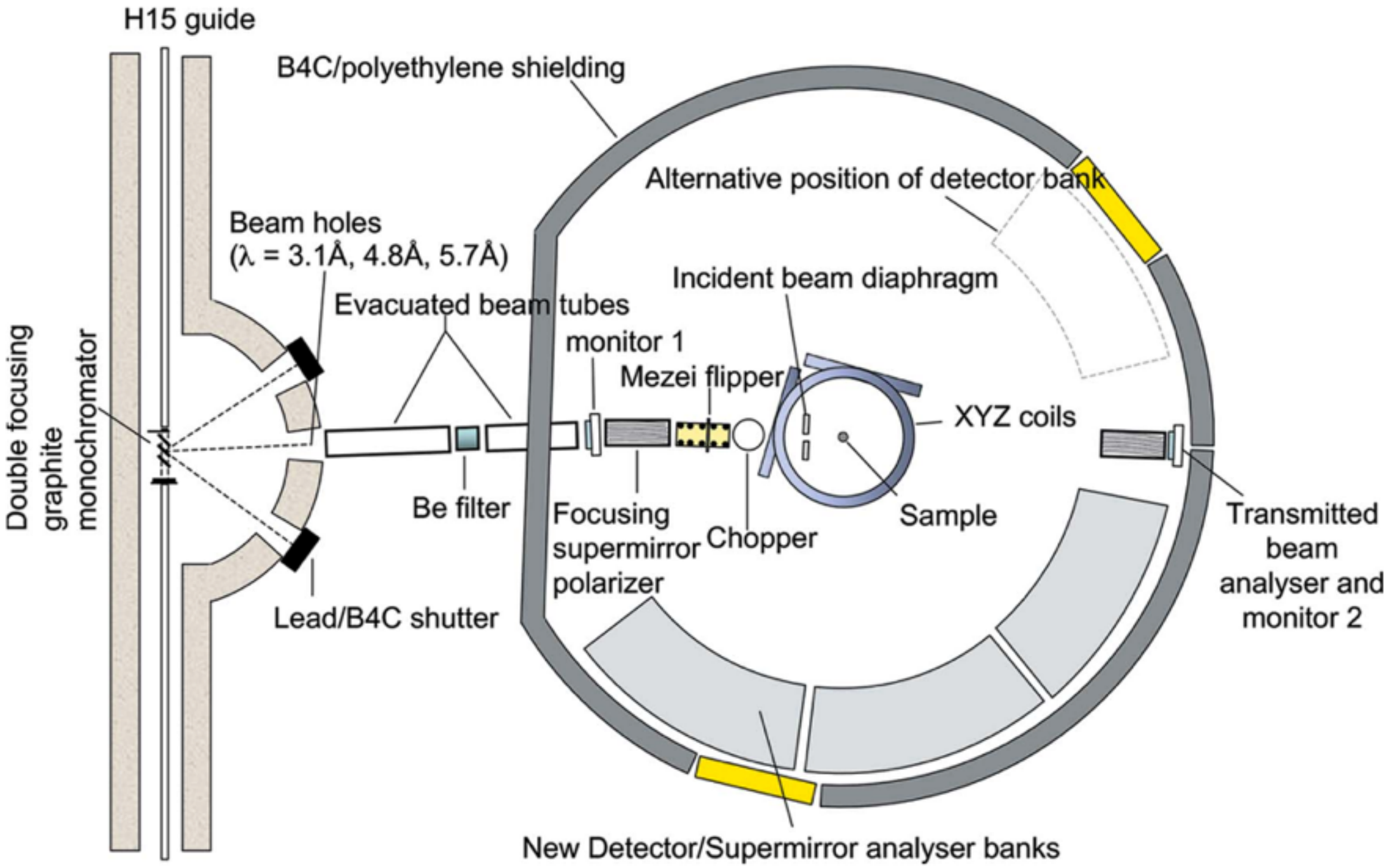


**Figure 2**
The diffuse scattering spectrometer D7 of the ILL.

# TOF distinguishes elastic from diffuse scattering
# Co/Ti “super-mirrors” magnetized to detect spin flip

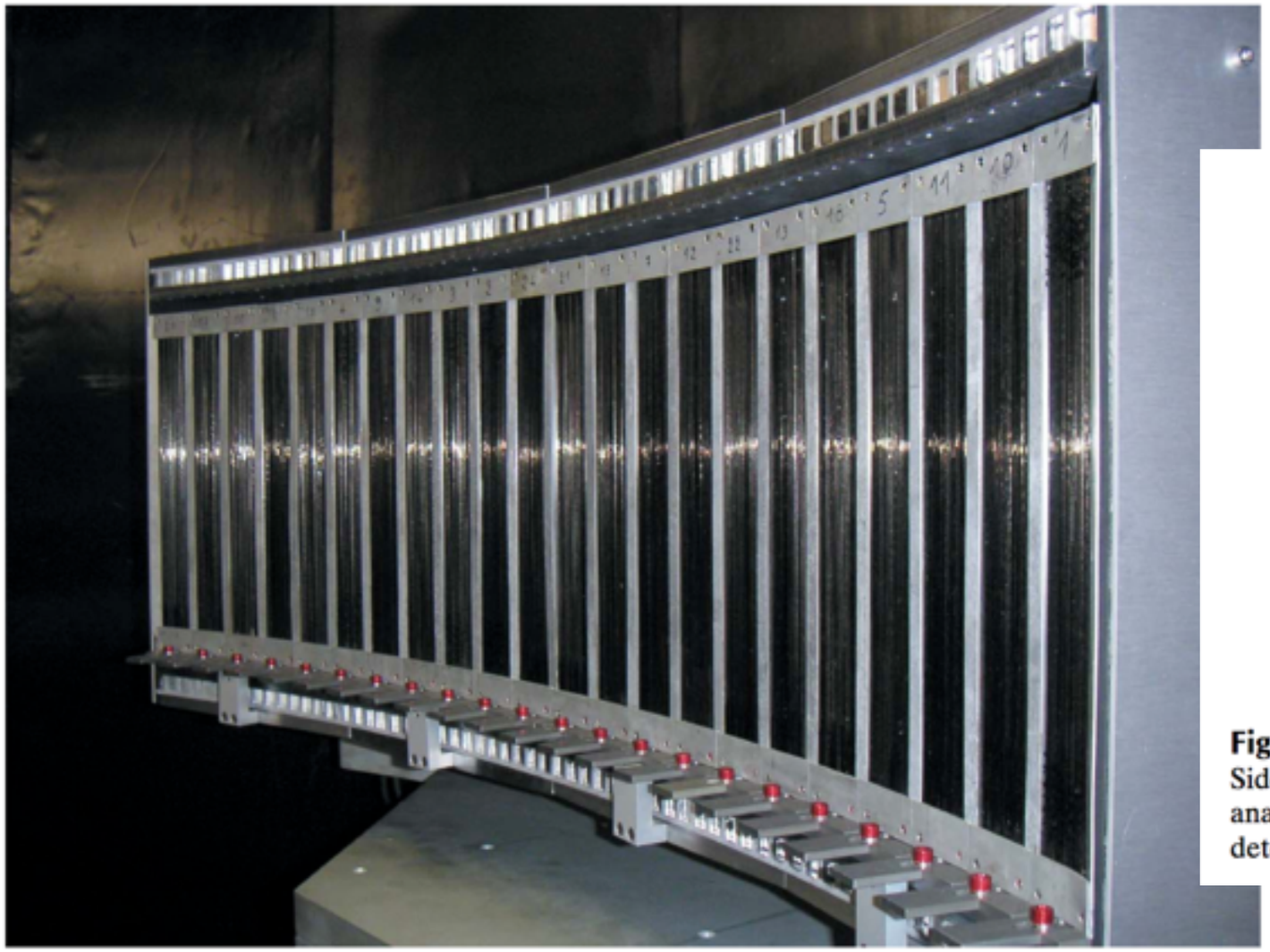

**Figure 11**
Analyser bank upon installation. At the top it is possible to distinguish the NdFeB magnets.

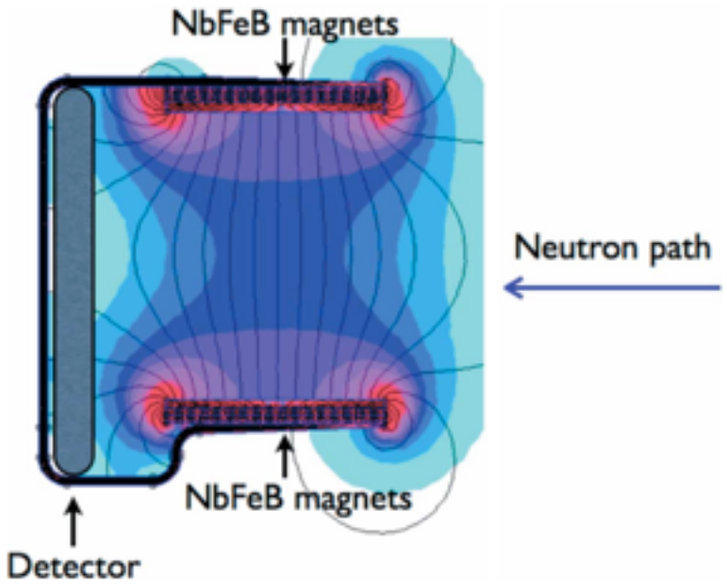


**Figure 10**
Side view of the magnetic holding fields around the supermirror analysers. The ferromagnetic yoke creates a return field behind the detector.

aleatory (random)

We now describe the information provided by the diffraction experiments with polarization analysis. Contrarily to the coherent scattering, which does not induce a spin flip, incoherent scattering of a sample constituted of aleatory oriented spins has a 2/3 probability to spin flip the scattered neutrons. Hence the separation of incoherent and coherent nuclear scattering processes can be achieved using a polarized incident neutron beam and counting separately the neutrons scattered with and without spin-flip with regard to the incident beam polarization [1]. Two different $Q$-dependent intensities are obtained: the spin flip intensity $I_{SF}(Q)$ and the non-spin flip intensity $I_{NSF}(Q)$. From these, the ratio between the coherent and incoherent scattering cross sections can easily be calculated:

$$\frac{\left(\frac{\partial\sigma}{\partial\Omega}\right)_{coh}(Q)}{\left(\frac{\partial\sigma}{\partial\Omega}\right)_{inc}(Q)} = \frac{I_{NSF}(Q) - \frac{1}{2}I_{SF}(Q)}{\frac{3}{2}I_{SF}(Q)}. \tag{S3}$$

This procedure has the advantage to directly correct the coherent scattering function from Debye-Waller factor (DWF) and instrumental effects.

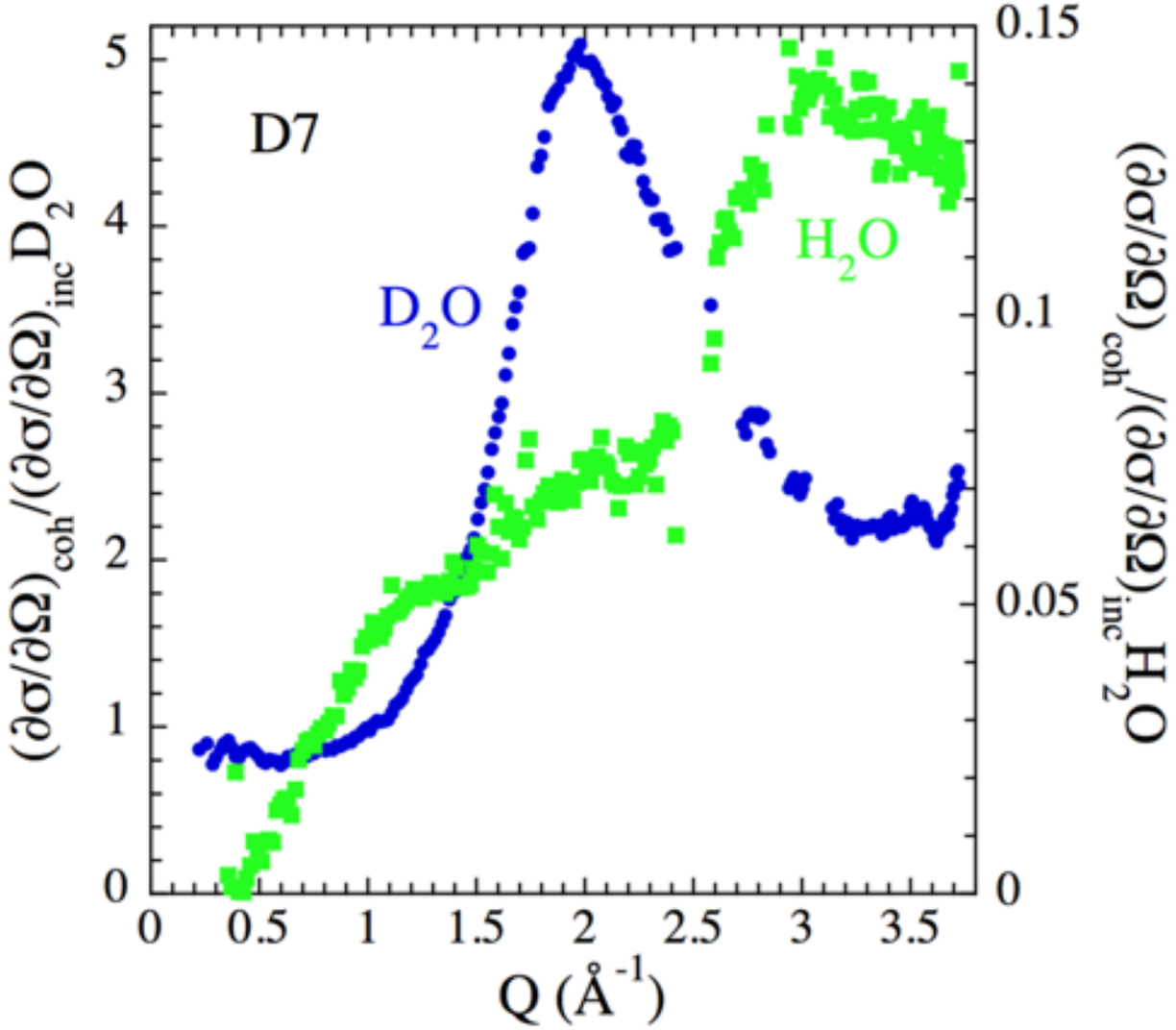


Figure S1 shows the D7 experimental results on $D_2O$ and $H_2O$. The $Q \to \infty$ limit of the ratio represented in this figure is determined by the ratio of the coherent and incoherent cross sections. From the above given values, these ratios would theoretically amount to $\sigma_{coh}^{D_2O}/\sigma_{inc}^{D_2O} = 3.76$ and $\sigma_{coh}^{H_2O}/\sigma_{inc}^{H_2O} = 0.048$. As can be seen, the experimental data are compatible with such asymptotic values. Thus, the intensity scattered by $H_2O$ is completely dominated by the incoherent contribution from the hydrogens, while that scattered by $D_2O$ is predominantly of coherent nature above $\approx$1.5 Å$^{-1}$. At low $Q$-values, the incoherent contribution for this sample is about the same as the coherent one.

# coherent scattering measures atomic position correlation "S(Q,ν)"

By contrast, neutrons interact directly with atomic nuclei. A neutron scattering experiment (see Fig. 1) can measure both local atomic motions and larger-scale collective dynamics. Neutron scattering determines the so-called dynamic structure factor, or $S(Q,\nu)$, as a function of frequency $\nu$ and momentum transfer $Q$, which correspond, respectively, to the differences of energy and momentum between incoming and outgoing neutrons. $S(Q,\nu)$ is a correlation function between positions occupied by the same or different atoms at different times. Spatial information on molecular dynamics can be derived from the $Q$ dependence, while temporal information can be accessed via the energy dependence.

# S(Q,v) directly related to dielectric susceptibility

Studies of liquid water that combine dielectric relaxation and neutron scattering have previously been carried out, but they amounted to qualitative observations. Arbe *et al.* now provide the first quantitative study using the two techniques. The observables in the two experiments— $\chi''(\nu)$ in dielectric relaxation and $S(Q,\nu)$ in neutron scattering—are directly related: $S(Q,\nu)$ can be connected to the dielectric susceptibility $\chi''(Q,\nu) = (\nu/k_BT) \cdot S(Q,\nu)$, where $k_B$ is the Boltzmann constant and $T$ is the absolute temperature. $\chi''(Q,\nu)$ is the equivalent of $\chi''(\nu)$, the imaginary part of the dielectric constant measured in dielectric relaxation.

$P = \epsilon_0 \chi E$ dielectric $\varepsilon = 1 + \chi$

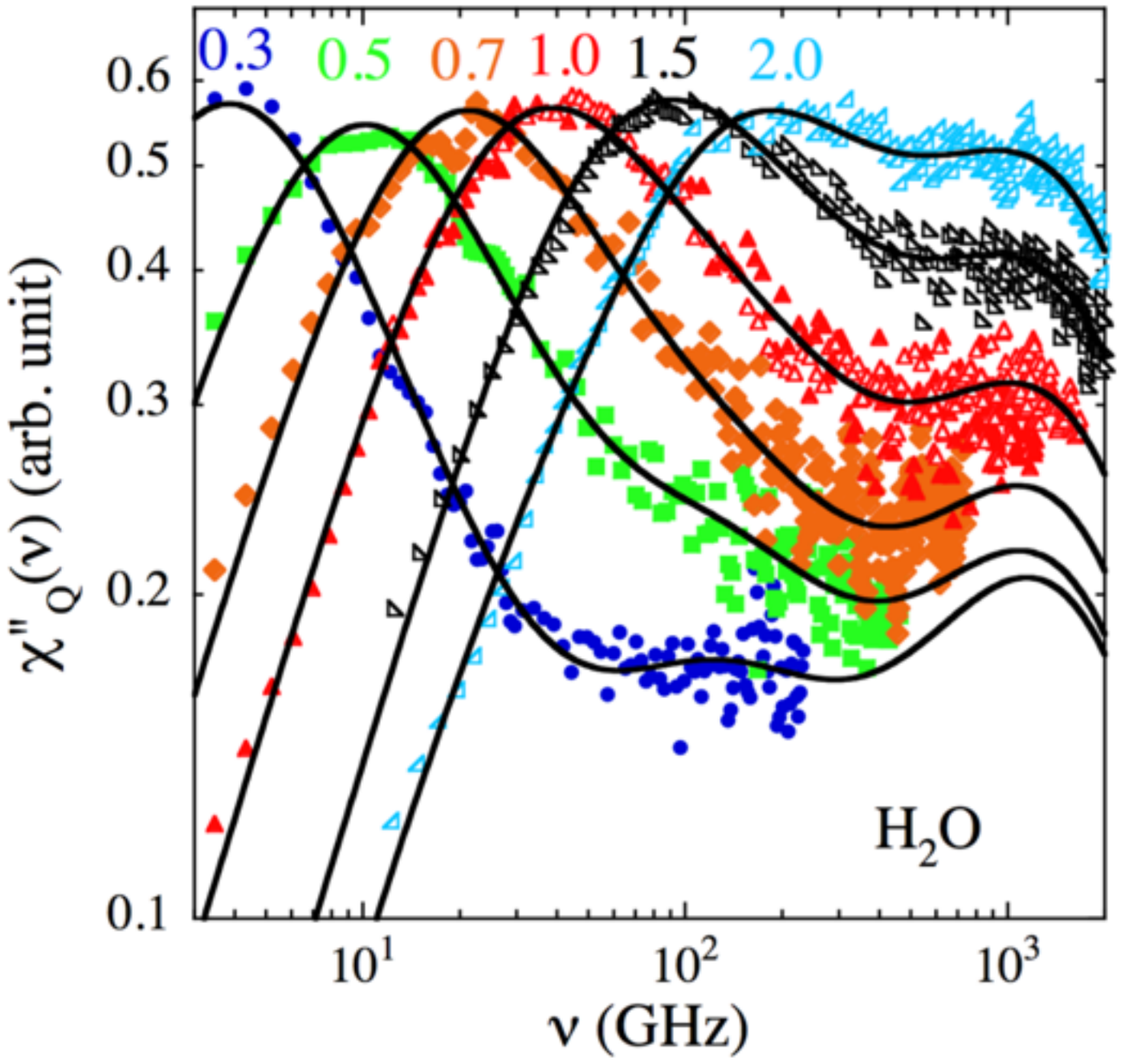


FIG. S2. Susceptibility curves obtained from the time-of-flight $H_2O$ results at the $Q$-values indicated (in $Å^{-1}$). Filled symbols correspond to results obtained with $\lambda$=8Å, empty symbols to $\lambda$=5Å. Solid lines are fits of the convolution model function with fixed $\tau_\ell$=1.3ps ($\Gamma_\ell = (2\pi\tau_\ell)^{-1}$=122GHz), $\nu_o^{H_2O}$=2.64THz and $k_o^{H_2O}$=38.7THz.

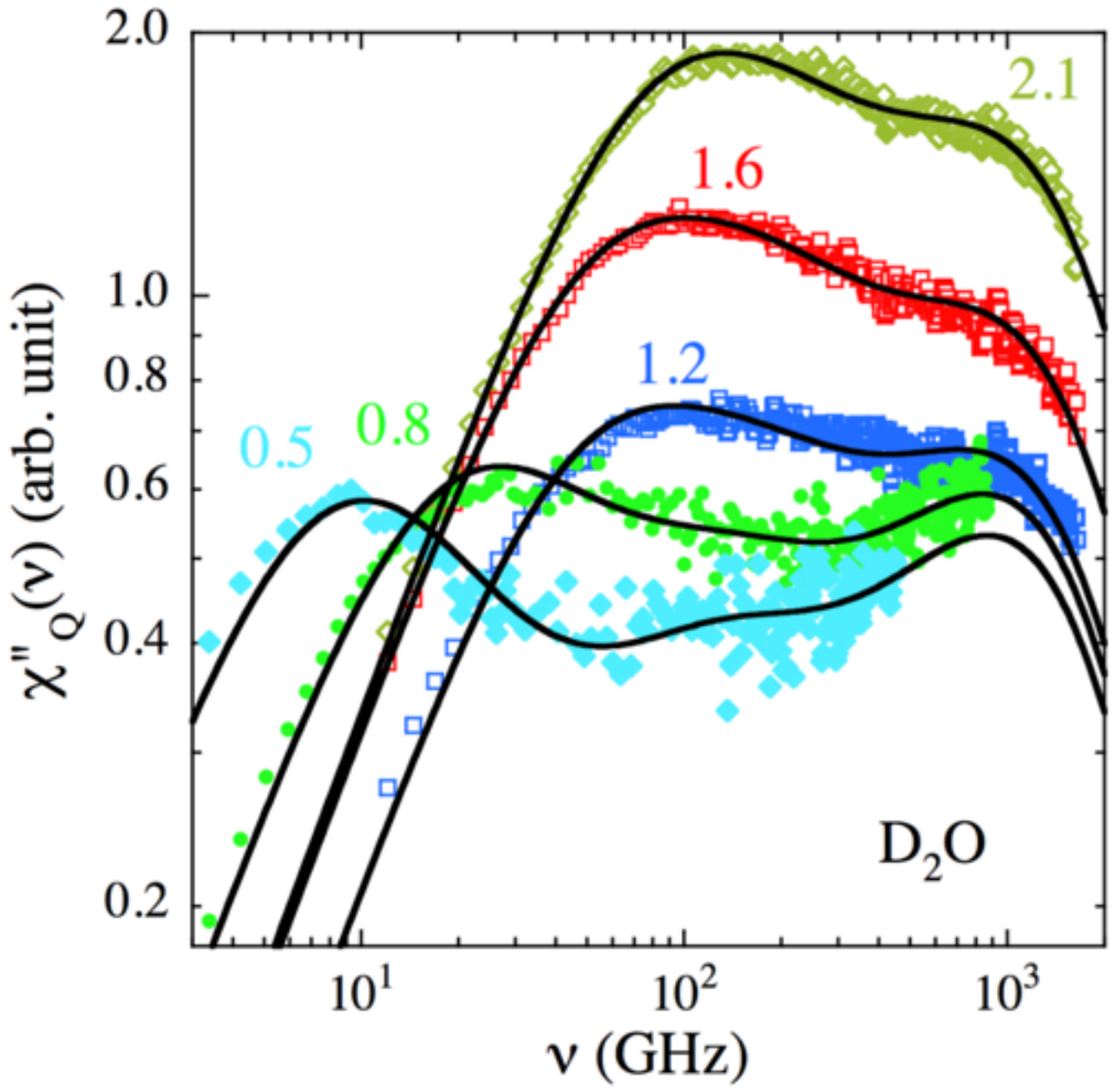


FIG. S3. Susceptibility curves obtained from the time-of-flight $D_2O$ results at the $Q$-values indicated (in $Å^{-1}$). Filled symbols correspond to results obtained with $\lambda$=8Å, empty symbols to $\lambda$=5Å. Solid lines are fits of the convolution model function with fixed $\tau_\ell$=1.3ps ($\Gamma_\ell = (2\pi\tau_\ell)^{-1}$=122GHz), $\nu_o^{D_2O}$=1.75THz and $k_o^{D_2O}$=22.5THz.

# 0.15 THz peak: 8 ps dynamics , Q = 0.7 Å

# dipolar relaxation due to long distance (0.34 nm) molecular diffusion

The main feature of dielectric relaxation measurements is a peak in $\varepsilon''(\nu)$ centered at 20 GHz. This is the well-known Debye peak, indicating that the collective relaxation of the macroscopic dipole moment occurs on a time scale of 8.3 ps (Fig. 2). Arbe and colleagues have now carried out coherent and incoherent neutron scattering experiments to shed new light on the molecular origin of this relaxation. The authors show that the same peak is seen in $H_2O$ when the (incoherent) neutron scattering susceptibility is measured at $Q = 7$ $nm^{-1}$. The $Q$ dependence of the peak position demonstrates that dipolar relaxation is linked to molecular diffusion and gives the length scale of collective dipolar relaxation. The researchers deduce that the 8.3-ps dynamics is due to the movement of atoms along relatively large distances (0.34 nm), which are comparable to or slightly larger than intermolecular distances.

# THz peak ($Q=2\text{Å}^{-1}$): H move in "cage" of size 0.05 nm

molecular distances.

Similarly to the study of dielectric relaxation [2], the authors' neutron scattering experiment also reveals two smaller peaks in the THz domain, a high-frequency range hardly accessible by dielectric relaxation. Because their position doesn't change with $Q$, the peaks correspond to localized motions. The peak at the highest frequency (around 2 THz) is associated with bending of chains of three oxygen molecules connected by hydrogen bonds (O—O—O). The other one, at intermediate frequencies (around 0.15 THz), is a novel finding of this work. This peak is related to local processes—motions of hydrogen atoms that take place when intermolecular bonds break and reform on picosecond time scales. By separating the contributions of oxygen and hydrogen atoms to scattering data, the researchers show that, on 0.1 to 1 ps time scales, the hydrogen atom moves in a "cage" with a size of 0.05 nm. Such a size corresponds to an amplitude of vibration or delocalization of hydrogens much smaller than the intermolecular distance, which is 0.28 nm on average.

# Oxygen motion

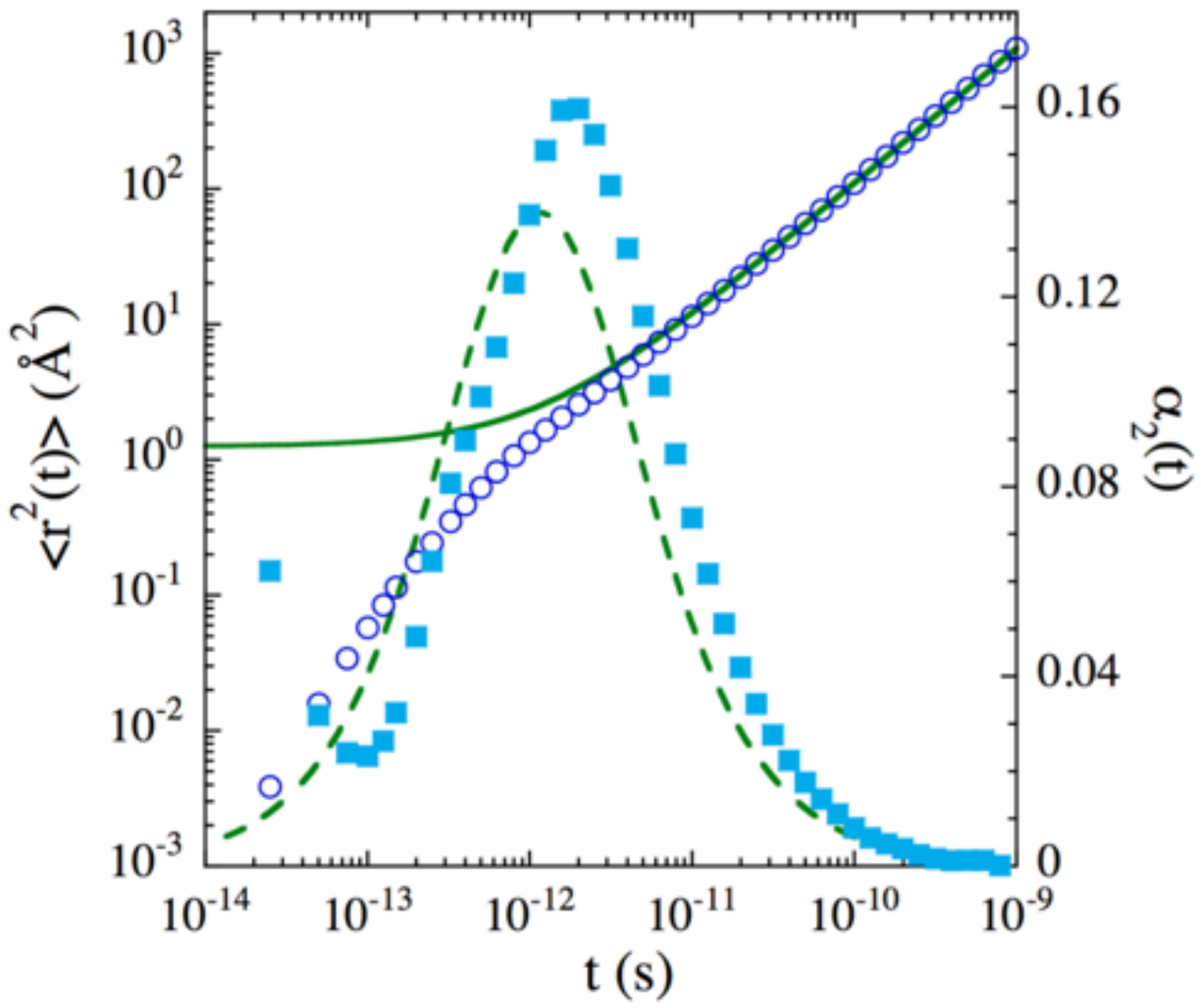


FIG. S7. Mean squared displacement (empty symbols) and non-Gaussian parameter (solid symbols) of oxygens obtained from the MD-simulations. Lines are fits of Eqs. S13 and S14 with $l$=0.59Å and $\tau_0$=0.32ps (as deduced from the description of the $Q$-dependence of the characteristic time, see Fig. S6). The value deduced for $\langle u^2 \rangle$ is 0.62Å$^2$.

future work: various Temperatures